

# Physical Chemistry

## Structural parameters of concentrated aqueous solutions of LiCl under extreme conditions, as calculated by the method of integral equations. Effect of temperature

R. D. Oparin,\* M. V. Fedotova, and V. N. Trostin

*Institute of Solution Chemistry, Russian Academy of Sciences,  
1 ul. Akademicheskaya, 153045 Ivanovo, Russian Federation.  
Fax: +7 (093 2) 37 8509. E-mail: adm@ihnr.polytech.ivanovo.su*

Peculiarities of structure formation of aqueous LiCl solutions at different salt : water molar ratios (LiCl :  $n$  H<sub>2</sub>O,  $n = 3.15, 8.05, 14.90$ ) under conditions of isobaric heating ( $p = 100$  bar,  $T = 298, 323–523$  K,  $\Delta T = 50$  K) were studied by the method of integral equations. Heating of LiCl : 14.90H<sub>2</sub>O solution was found to lead to disappearance of tetrahedral ordering of solvent molecules, appreciable weakening of the coordination abilities of both ions, and to an increase of the number of contact ion pairs and a decrease of the number of solvent-separated ion pairs. For the LiCl : 8.05H<sub>2</sub>O system, the tetrahedral structure of the solvent disappears at a lower temperature and heating has a less pronounced effect on the coordination and associative abilities of the ions. In the LiCl : 3.15H<sub>2</sub>O solution, tetrahedral ordering of the solvent molecules disappears at 298 K and the number of contact ion pairs decreases as temperature increases. Other structural changes in this system upon heating are similar to those found for the LiCl : 14.90H<sub>2</sub>O and LiCl : 8.05H<sub>2</sub>O solutions.

**Key words:** integral equation method, pair correlation functions, lithium chloride, aqueous solutions, structural parameters, high temperature.

Studies of structural properties of water-electrolyte systems at high pressures and temperatures have drawn considerable recent attention of researchers in the context of the development of advanced technologies involving hydrothermal oxidation of chemical waste and hydrothermal synthesis.

In spite of topicality of this investigation line, only a few studies on the structural characteristics of water and aqueous electrolyte solutions at extreme state parameters have been reported to date.<sup>1–13</sup> This is due to two reasons, namely, difficulties in performing experiments

under extreme conditions and relatively time-consuming computer simulation. Fortunately, there is a class of theoretical approaches including the method of integral equations (IE) employed in this work, which also allows the description of various properties of water-electrolyte systems (ionic solvation, interionic interactions, character of short-range ordering of ions, *etc.*) and represents a "third avenue" of research in addition to experimental studies and computer simulation. In the framework of the IE method, structural and thermodynamic characteristics of the objects under study are calculated based

on the known potentials of interparticle interactions. Similarly to direct structural approaches, the IE method allows the description of diffusion-averaged structure of liquid-phase systems, thus being different from computer simulation methods (molecular dynamics, MD, and Monte Carlo, MC). In addition, calculations of structural parameters of solutions using the IE method are much less time consuming compared to MD and MC simulation.

Structural parameters obtained using the IE method are in reasonable agreement with the results of experimental studies and those obtained from MD and MC simulation at standard state parameters. Up to now, the IE method has mainly been used in studies of water and aqueous electrolyte solutions under standard conditions, whereas studies on the structure of these objects under extreme conditions can be counted on the fingers of one hand.<sup>14–16</sup> Usually, the authors do not consider the dynamics of structural changes in the systems on going from standard to extreme state parameters. Moreover, most of them often do not analyze interionic interactions which play an important role in the structure formation of concentrated aqueous salt systems.

This work was carried out in a continuation of our studies of the structure of aqueous electrolyte (1 : 1) solutions under extreme conditions.<sup>17–20</sup> It concerns the effect of temperature on the structure of aqueous LiCl solutions of three concentrations (LiCl :  $n$  H<sub>2</sub>O,  $n$  = 3.15, 8.05, and 14.90) at constant pressure. Structural parameters of the systems under study were calculated for  $p$  = 100 bar and  $T$  = 298 K and for the temperature range from 323 up to 523 K with an increment ( $\Delta T$ ) of 50 K.

### Calculation Procedure

In the course of simulation the solutions under study were represented as mixtures of water molecules and ions. Ion–water and ion–ion interactions were described by pair potentials.<sup>21</sup> A modified TIPS model<sup>22</sup> with the known parameters<sup>23</sup> was used for water. These potentials of interparticle interactions and water model were chosen since they are (i) computationally simple and (ii) thought to be efficient for the description of the structure of water-electrolyte systems.

Calculations of structural parameters were performed using the Ornstein–Zernike atom-atom integral equation.<sup>24</sup> In the case of ion-molecular systems it is represented by a system of three equations describing solvent–solvent (W–W), solute–solvent (I–W), and solute–solute (I–I) correlations:

$$\begin{aligned} \rho_W \mathbf{h}_{WW}(k) &= \mathbf{s}_{WW}(k) \mathbf{c}_{WW}(k) \mathbf{s}_{WW}(k) + \\ &+ \rho_W \mathbf{s}_{WW}(k) \mathbf{c}_{WW}(k) \mathbf{h}_{WW}(k), \\ \mathbf{h}_{IW}(k) &= \mathbf{c}_{IW}(k) \mathbf{s}_{WW}(k) + \rho_W \mathbf{c}_{IW}(k) \mathbf{h}_{WW}(k), \\ \mathbf{h}_{II}(k) &= \mathbf{c}_{II}(k) + \rho_W \mathbf{c}_{IW}(k) \mathbf{h}_{IW}(k) + \rho_I \mathbf{c}_{II}(k) \mathbf{h}_{II}(k), \end{aligned} \quad (1)$$

where  $\rho_W$  is the density of solvent molecules;  $\rho_I$  is the density of ions; and  $\mathbf{h}_{\alpha\beta}(k)$ ,  $\mathbf{c}_{\alpha\beta}(k)$ , and  $\mathbf{s}_{\alpha\beta}(k)$  are matrices with the elements

$$\begin{aligned} \mathbf{h}_{\alpha\beta}^{xy}(k) &= \frac{4\pi}{k} \sqrt{\rho_x \rho_y} \int_0^\infty r dr h_{\alpha\beta}^{xy}(r) \sin(kr), \\ \mathbf{c}_{\alpha\beta}^{xy}(k) &= \frac{4\pi}{k} \sqrt{\rho_x \rho_y} \int_0^\infty r dr c_{\alpha\beta}^{xy}(r) \sin(kr), \\ \mathbf{s}_{\alpha\beta}^{xy}(k) &= \delta_{xy} \left[ \delta_{\alpha\beta} + (1 - \delta_{\alpha\beta}) \frac{\sin(kl_{\alpha\beta}^x)}{kl_{\alpha\beta}^x} \right], \end{aligned}$$

where  $\rho_x$  is the density of the molecules of sort  $x$ ;  $\rho_y$  is the density of the molecules of sort  $y$ ;  $l_{\alpha\beta}$  is the distance between the force centers  $\alpha$  and  $\beta$  belonging to the molecule of sort  $x$ ;  $h_{\alpha\beta}^{xy}(r)$  and  $c_{\alpha\beta}^{xy}(r)$  is respectively the total and direct atom-atom correlation function of the force centers  $\alpha$  (for molecule  $x$ ) and  $\beta$  (for molecule  $y$ );  $\mathbf{s}_{\alpha\beta}^{xy}(r)$  is the matrix of Fourier-transforms of the function describing intramolecular correlations;  $\delta_{xy}$  is the Dirac delta function; and  $\delta_{\alpha\beta}$  is the Kronecker delta.

The hypernetted chain closure was used for the system of equations (1):

$$\begin{aligned} h_{WW}(r) + 1 &\equiv g_{WW}(r) = \\ &= \exp[-BU_{WW}(r) + h_{WW}(r) - c_{WW}(r)], \\ h_{IW}(r) + 1 &\equiv g_{IW}(r) = \exp[-BU_{IW}(r) + h_{IW}(r) - c_{IW}(r)], \\ h_{II}(r) + 1 &\equiv g_{II}(r) = \exp[-BU_{II}(r) + h_{II}(r) - c_{II}(r)], \end{aligned} \quad (2)$$

where  $g(r) \equiv g_{\alpha\beta}^{xy}(r)$  is the pair atom-atom correlation function (PCF) of the force centers  $\alpha$  and  $\beta$  belonging to the molecules  $x$  and  $y$ , respectively;  $-BU(r) \equiv -BU_{\alpha\beta}^{xy}(r) = -B[\Phi_{\alpha\beta}^{xy}(r) + \Phi_{\alpha\beta}^{xy}(r)]$  is the initial potential of the atom-atom interaction (the functions  $\Phi_{\alpha\beta}^{xy}(r)$  and  $\Phi_{\alpha\beta}^{xy}(r)$  describe short-range and long-range interactions, respectively);  $B = (k_B T)^{-1}$ ; and  $k_B$  is the Boltzmann constant.

The solution of the Ornstein–Zernike atom-atom IE for the system with a long-range electrostatic interaction requires renormalization of the initial long-range potential in such a way that only the renormalized shielded potential describing the long-range interaction appeared in the equation. The scheme of this procedure, as well as the method of numerical solution of the Ornstein–Zernike atom-atom IE with the hypernetted chain closure have been reported previously.<sup>25</sup> The main idea of the method is to combine the Picard direct iteration approach and the Newton–Raphson scheme to solve the system of nonlinear equations.

Our calculations by the IE method made it possible to obtain the  $g_{\alpha\beta}(r)$  PCF for the aqueous LiCl solutions under study and use them for determination of the interparticle distances, presence and type of ionic associates in the solutions, as well as coordination numbers of the particles,

$$n_{\alpha\beta}(r) = 4\pi \rho_\beta \int_0^r g_{\alpha\beta}(r) r^2 dr,$$

where  $\rho_\beta$  is the density of particles of the sort  $\beta$  ( $\text{\AA}^{-3}$ ) coordinated by the particle of the sort  $\alpha$ . Based on the relative changes in the  $\Delta n_{\alpha\beta}(r_{m1})$  values, we analyzed the changes in the structural parameters of the solvent and the associative and coordination ability of ions as functions of external state parameters:

$$\Delta n_{\alpha\beta}(r_{m1}) = \frac{n_{\alpha\beta}^T(r_{m1}) - n_{\alpha\beta}^{298}(r_{m1})}{n_{\alpha\beta}^{298}(r_{m1})} \cdot 100\%,$$

where  $n_{\alpha\beta}^T(r_{m1})$  is the coordination numbers of the particle at a temperature  $T$  ( $T \neq 298$  K);  $r_{m1}$  is the first minimum position of

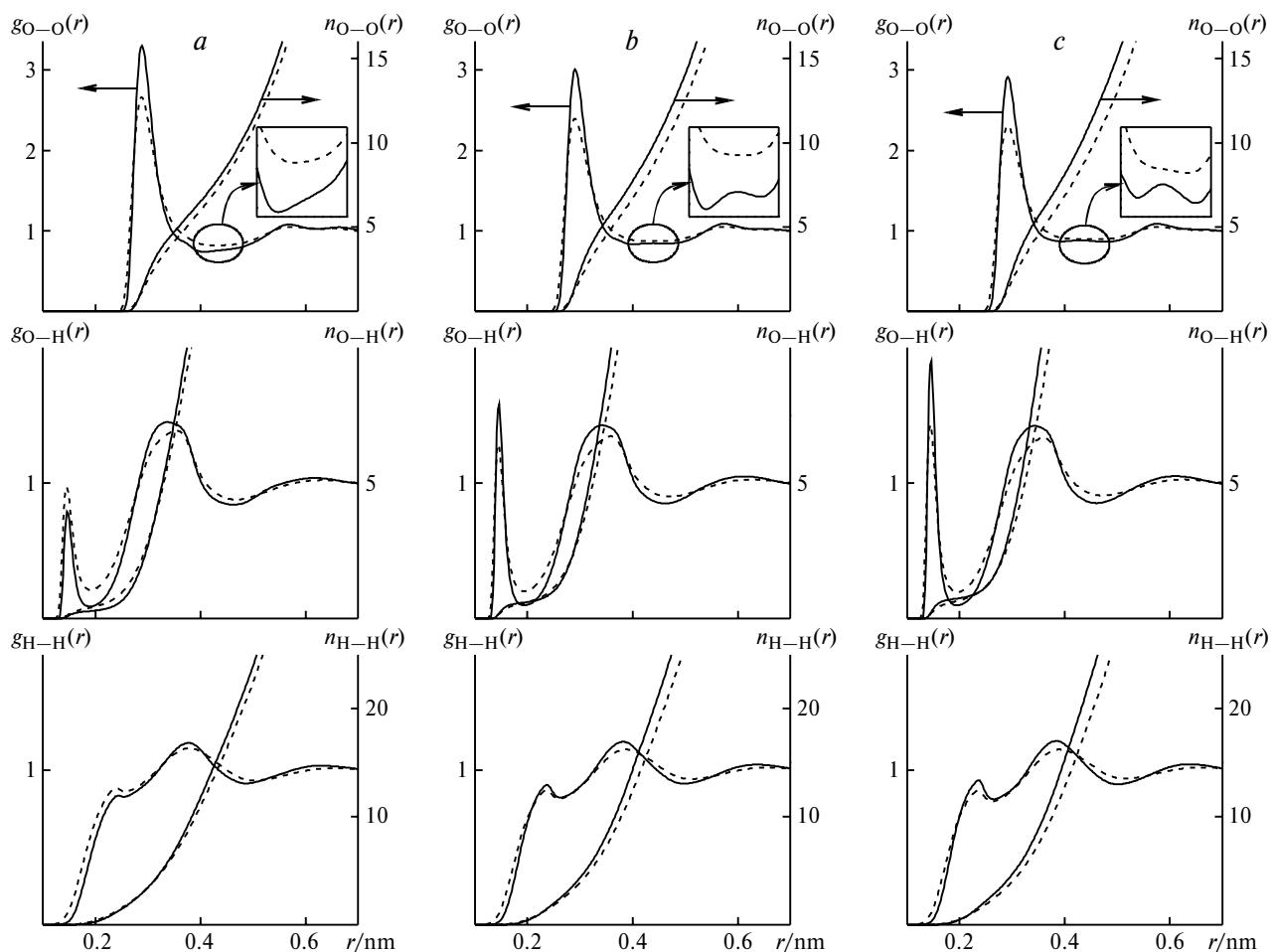


**Fig. 1.** Pair correlation functions  $g_{W-W}(r)$  and  $n_{W-W}(r)$  of LiCl : 3.15 H<sub>2</sub>O (a), LiCl : 8.05 H<sub>2</sub>O (b), and LiCl : 14.90 H<sub>2</sub>O (c) solutions calculated for  $T = 298$  K (solid line) and 523 K (dashed line).

the  $g_{\alpha\beta}(r)$  PCF. In solving the Ornstein-Zernike atom-atom IE the accuracy of both direct and Newton-Raphson iterations was  $10^{-3}$ . The coordination numbers of the particles were estimated with an accuracy of  $10^{-2}$ .

## Results and Discussion

Figures 1–3 present the plots of the  $g_{\alpha\beta}(r)$  and  $n_{\alpha\beta}(r)$  PCF obtained only for the lowest (298 K) and highest (523 K) temperature since the characteristic values of these functions were found to be close. The characteristic values of other PCF for the whole temperature range are listed in Tables 1–3.

### Water–water ( $W-W$ ) correlations

According to calculations for  $T = 298$  K, the main peak of the  $g_{O-O}(r)$  PCF is at  $r_{M1} = 0.292$  nm for LiCl : 14.90 H<sub>2</sub>O and at 0.290 nm for LiCl : 8.05 H<sub>2</sub>O (see Fig. 1). These peaks are determined by the interactions between water molecules and the nearest environment. The second maximum, at  $r_{M2} = 0.432$  (LiCl : 14.90 H<sub>2</sub>O) and 0.440 nm (LiCl : 8.05 H<sub>2</sub>O), is

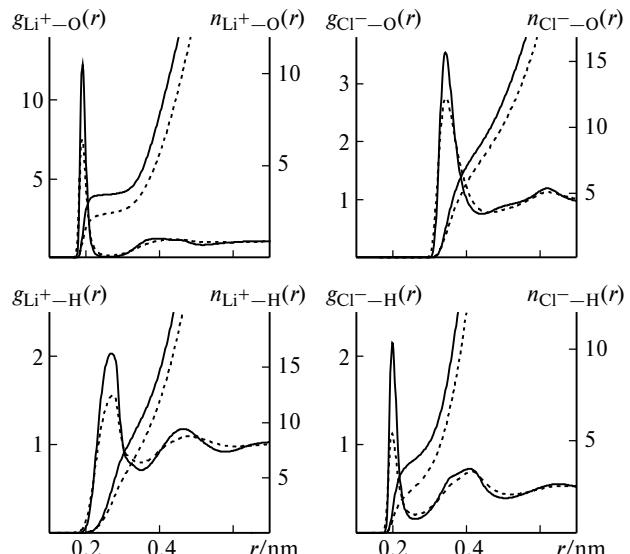


**Fig. 2.** Pair correlation functions  $g_{I-W}(r)$  and  $n_{I-W}(r)$  of the LiCl : 14.90 H<sub>2</sub>O solution calculated for  $T = 298$  K (solid line) and 523 K (dashed line).

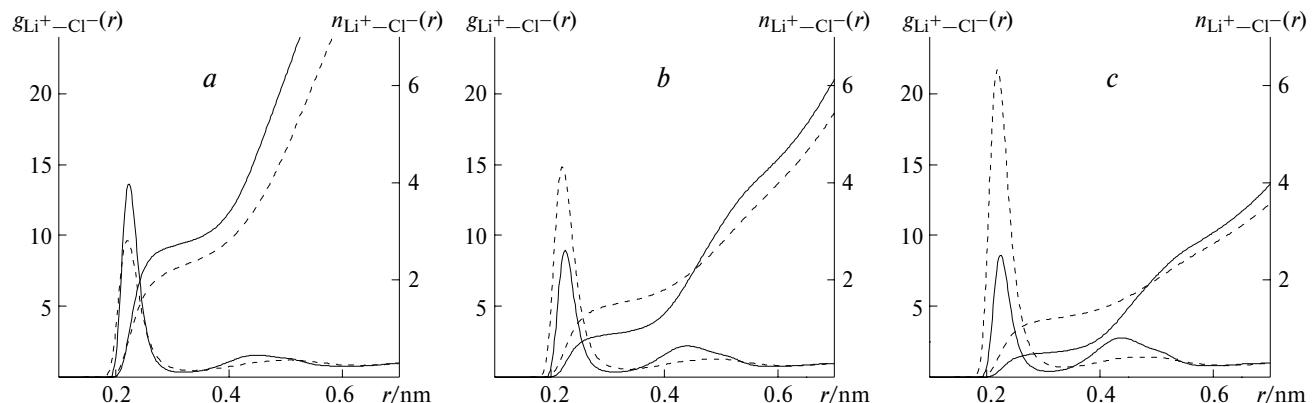


**Fig. 3.** Pair correlation functions  $g_{\text{Li}^+ - \text{Cl}^-}(r)$  and  $n_{\text{Li}^+ - \text{Cl}^-}(r)$  of the  $\text{LiCl} : 3.15 \text{ H}_2\text{O}$  (a),  $\text{LiCl} : 8.05 \text{ H}_2\text{O}$  (b), and  $\text{LiCl} : 14.90 \text{ H}_2\text{O}$  (c) solution calculated for  $T = 298 \text{ K}$  (solid line) and  $523 \text{ K}$  (dashed line).

due to the interactions between water molecules in the tetrahedral structure. The peak in the region  $0.570$ – $0.580 \text{ nm}$  is determined by the interactions between these water molecules and more distant molecules. This shape of the  $g_{\text{O} - \text{O}}(r)$  PCF is also typical of neat water, which is in good agreement with the results of experimental studies (see, e.g., Refs. 26–28).

From the plots shown in Fig. 1 and data listed in Table 1 it can be seen that heating of the  $\text{LiCl} : 14.90 \text{ H}_2\text{O}$  solution causes a substantial decrease in the main peak intensity of  $g_{\text{O} - \text{O}}(r)$ . However, position of this peak remains unchanged. In the temperature

range  $298$ – $423 \text{ K}$ , the first minimum of this PCF is appreciably shifted toward longer  $r$  and becomes shallower. Simultaneously, the intensity of the second peak at  $r_{\text{M}2} = 0.432 \text{ nm}$  decreases and the second maximum and minimum are shifted toward shorter  $r$ , the latter becoming shallower. These changes in the  $g_{\text{O} - \text{O}}(r)$  shape lead to a decrease in the number of tetrahedrally ordered water molecules (the  $n^{(\text{II})}_{\text{O} - \text{O}}(r_{\text{M}2})$  value reduces by more than 33%) and a fraction of them appears to constituents of the nearest environment, which corresponds to a 5.1% increase in the  $n^{(\text{I})}_{\text{O} - \text{O}}(r_{\text{M}1})$  value.

**Table 1.** Characteristic values of the  $g_{\alpha\beta}(r)$  PCF and  $n_{\alpha\beta}(r)$  functions for the  $\text{LiCl} : 14.90 \text{ H}_2\text{O}$  system under isobaric heating ( $p = 100 \text{ bar}$ )

Parameter	298 K	323 K	373 K	423 K	473 K	523 K
$g_{\text{O} - \text{O}}(r_{\text{M}1})$	2.916 (0.292)	2.831 (0.292)	2.680 (0.292)	2.544 (0.292)	2.418 (0.292)	2.306 (0.292)
$g_{\text{O} - \text{O}}(r_{\text{m}1})$	0.871 (0.394)	0.873 (0.398)	0.880 (0.404)	0.887 (0.412)	— <sup>a</sup>	— <sup>a</sup>
$n^{(\text{I})}_{\text{O} - \text{O}}(r_{\text{m}1})$	7.79 (0.394)	7.93 (0.398)	8.03 (0.404)	8.19 (0.412)	— <sup>a</sup>	— <sup>a</sup>
$g_{\text{O} - \text{O}}(r_{\text{M}2})$	0.886 (0.432)	0.884 (0.430)	0.884 (0.430)	0.888 (0.428)	— <sup>a</sup>	— <sup>a</sup>
$g_{\text{O} - \text{O}}(r_{\text{m}2})$	0.865 (0.478)	0.868 (0.476)	0.875 (0.472)	0.882 (0.470)	0.890 (0.468)	0.899 (0.468)
$n^{(\text{II})}_{\text{O} - \text{O}}(r_{\text{m}2})$	5.50 (0.478)	5.08 (0.476)	4.36 (0.472)	3.68 (0.470)	— <sup>a</sup>	— <sup>a</sup>
$n^{(\text{I}+\text{II})}_{\text{O} - \text{O}}(r_{\text{m}2})$	13.29 (0.478)	13.01 (0.476)	12.39 (0.472)	11.87 (0.470)	11.27 (0.468)	10.75 (0.468)
$g_{\text{O} - \text{H}}(r_{\text{M}1})$	1.897 (0.146)	1.815 (0.146)	1.674 (0.144)	1.578 (0.144)	1.501 (0.144)	1.433 (0.144)
$g_{\text{O} - \text{H}}(r_{\text{m}1})$	0.097 (0.194)	0.112 (0.196)	0.138 (0.196)	0.160 (0.196)	0.179 (0.196)	0.195 (0.196)
$n_{\text{O} - \text{H}}(r_{\text{m}1})$	0.73 (0.194)	0.73 (0.196)	0.72 (0.196)	0.70 (0.196)	0.68 (0.196)	0.65 (0.196)
$g_{\text{Li}^+ - \text{Cl}^-}(r_{\text{M}1})$	8.609 (0.224)	11.223 (0.224)	15.930 (0.222)	17.911 (0.222)	19.948 (0.220)	21.732 (0.220)
$g_{\text{Li}^+ - \text{Cl}^-}(r_{\text{m}1})$	0.401 (0.310)	0.478 (0.314)	0.588 (0.320)	0.638 (0.326)	0.670 (0.332)	0.701 (0.338)
$n^{(\text{I})}_{\text{Li}^+ - \text{Cl}^-}(r_{\text{m}1})$	0.50 (0.310)	0.66 (0.314)	0.93 (0.320)	1.06 (0.326)	1.16 (0.332)	1.24 (0.338)
$g_{\text{Li}^+ - \text{Cl}^-}(r_{\text{M}2})$	2.767 (0.438)	2.451 (0.440)	1.975 (0.442)	1.654 (0.448)	1.475 (0.458)	1.398 (0.470–0.480)
$g_{\text{Li}^+ - \text{Cl}^-}(r_{\text{M}2'})$	2.171–1.353 (0.480–0.530) <sup>b</sup>	2.012–1.307 (0.480–0.530) <sup>b</sup>	1.750–1.232 (0.480–0.530) <sup>b</sup>	1.557–1.190 (0.480–0.530) <sup>b</sup>	1.444–1.185 (0.480–0.530) <sup>b</sup>	— <sup>a</sup>
$g_{\text{Li}^+ - \text{Cl}^-}(r_{\text{m}2})$	0.796 (0.590)	0.787 (0.594)	0.779 (0.598)	0.784 (0.604)	0.802 (0.610)	0.831 (0.620)
$n^{(\text{II})}_{\text{Li}^+ - \text{Cl}^-}(r_{\text{m}2})$	2.40 (0.590)	2.25 (0.594)	1.98 (0.598)	1.78 (0.604)	1.67 (0.610)	1.64 (0.620)

*Note.*  $r_{\text{M}}$  is the position of maximum of the peak,  $g_{\alpha\beta}(r_{\text{M}})$  is the height of the peak;  $r_{\text{m}}$  is the position of minimum of the function;  $g_{\alpha\beta}(r_{\text{m}})$  is the function value at the minimum;  $n_{\alpha\beta}(r_{\text{m}})$  is the number of particles of the sort  $\beta$  at the distance  $r_{\text{m}}$  from the particle of the sort  $\alpha$ . The distances are given in nm.

<sup>a</sup> Not defined.

<sup>b</sup> The intervals of the function values (upper line) corresponding to the boundaries of the shoulders and diffuse peaks (lower line, figures in parentheses).

**Table 2.** Characteristic values of the  $g_{\alpha\beta}(r)$  PCF and  $n_{\alpha\beta}(r)$  functions for the LiCl : 8.05 H<sub>2</sub>O system under isobaric heating ( $p = 100$  bar)

Parameter	298 K	323 K	373 K	423 K	473 K	523 K
$g_{O-O}(r_{M1})$	3.007 (0.290)	2.925 (0.290)	2.773 (0.290)	2.635 (0.290)	2.510 (0.290)	2.396 (0.290)
$g_{O-O}(r_{m1})$	0.836 (0.402)	0.839 (0.404)	0.849 (0.408)	0.859 (0.414)	0.869 (0.426)	0.878 (0.448)
$n^{(I)}_{O-O}(r_{m1})$	7.81 (0.402)	7.84 (0.404)	7.86 (0.408)	7.93 (0.414)	8.28 (0.426)	9.17 (0.448)
$g_{O-O}(r_{M2})$	0.849 (0.440)	0.849 (0.442)	0.851–0.854 (0.420–0.460) <sup>b</sup>	— <sup>a</sup>	— <sup>a</sup>	— <sup>a</sup>
$g_{O-O}(r_{m2})$	0.846 (0.468)	0.848 (0.464)	— <sup>a</sup>	— <sup>a</sup>	— <sup>a</sup>	— <sup>a</sup>
$n^{(II)}_{O-O}(r_{m2})$	3.90 (0.468)	3.51 (0.464)	— <sup>a</sup>	— <sup>a</sup>	— <sup>a</sup>	— <sup>a</sup>
$g_{O-H}(r_{M1})$	1.584 (0.146)	1.533 (0.146)	1.456 (0.146)	1.386 (0.144)	1.333 (0.144)	1.287 (0.144)
$g_{O-H}(r_{m1})$	0.097 (0.194)	0.112 (0.194)	0.139 (0.194)	0.163 (0.194)	0.182 (0.194)	0.199 (0.194)
$n_{O-H}(r_{m1})$	0.59 (0.194)	0.59 (0.194)	0.59 (0.194)	0.59 (0.194)	0.58 (0.194)	0.57 (0.194)
$g_{Li^+-Cl^-}(r_{M1})$	8.948 (0.224)	10.901 (0.224)	12.558 (0.222)	13.747 (0.222)	14.393 (0.220)	14.864 (0.220)
$g_{Li^+-Cl^-}(r_{m1})$	0.350 (0.312)	0.404 (0.316)	0.472 (0.322)	0.514 (0.328)	0.541 (0.332)	0.563 (0.336)
$n^{(I)}_{Li^+-Cl^-}(r_{m1})$	0.89 (0.312)	1.10 (0.316)	1.30 (0.322)	1.44 (0.328)	1.52 (0.332)	1.56 (0.336)
$g_{Li^+-Cl^-}(r_{M2})$	2.200 (0.440)	1.973 (0.442)	1.615 (0.448)	1.405 (0.456)	1.287 (0.466–0.476) <sup>b</sup>	1.085–1.226 (0.430–0.470) <sup>b</sup>
$g_{Li^+-Cl^-}(r_{M2'})$	1.807–1.187 (0.480–0.530) <sup>b</sup>	1.695–1.163 (0.480–0.530) <sup>b</sup>	1.498–1.126 (0.480–0.530) <sup>b</sup>	1.368–1.110 (0.480–0.530) <sup>b</sup>	— <sup>a</sup>	1.249 (0.496)
$g_{Li^+-Cl^-}(r_{m2})$	0.740 (0.592)	0.743 (0.594)	0.751 (0.600)	0.767 (0.606)	0.788 (0.612)	0.813 (0.618)
$n^{(II)}_{Li^+-Cl^-}(r_{m2})$	3.50 (0.592)	3.31 (0.594)	3.01 (0.600)	2.81 (0.606)	2.69 (0.612)	2.64 (0.618)

Note. For notations, see Table 1.

**Table 3.** Characteristic values of the  $g_{\alpha\beta}(r)$  PCF and  $n_{\alpha\beta}(r)$  functions for the LiCl : 3.15 H<sub>2</sub>O system under isobaric heating ( $p = 100$  bar)

Parameter	298 K	323 K	373 K	423 K	473 K	523 K
$g_{O-O}(r_{M1})$	3.300 (0.288)	3.206 (0.288)	3.041 (0.288)	2.901 (0.288)	2.775 (0.288)	2.663 (0.288)
$g_{O-O}(r_{m1})$	0.743 (0.406)	0.755 (0.408)	0.774 (0.412)	0.792 (0.416)	0.808 (0.422)	0.823 (0.428)
$n^{(I)}_{O-O}(r_{m1})$	6.76 (0.406)	6.79 (0.408)	6.85 (0.412)	6.90 (0.416)	7.01 (0.422)	7.12 (0.428)
$g_{O-H}(r_{M1})$	0.790 (0.146)	0.870 (0.146)	0.940 (0.146)	0.969 (0.146)	0.976 (0.146)	0.969 (0.146)
$g_{O-H}(r_{m1})$	0.088 (0.190)	0.105 (0.190)	0.137 (0.190)	0.165 (0.190)	0.189 (0.190)	0.209 (0.190)
$n_{O-H}(r_{m1})$	0.27 (0.190)	0.30 (0.190)	0.34 (0.190)	0.37 (0.190)	0.38 (0.190)	0.39 (0.190)
$g_{Li^+-Cl^-}(r_{M1})$	13.655 (0.224)	12.010 (0.224)	11.470 (0.222)	10.762 (0.222)	10.129 (0.222)	9.654 (0.220)
$g_{Li^+-Cl^-}(r_{m1})$	0.334 (0.320)	0.355 (0.322)	0.395 (0.326)	0.424 (0.330)	0.447 (0.332)	0.467 (0.336)
$n^{(I)}_{Li^+-Cl^-}(r_{m1})$	2.76 (0.320)	2.54 (0.322)	2.52 (0.326)	2.50 (0.330)	2.42 (0.332)	2.37 (0.336)
$g_{Li^+-Cl^-}(r_{M2})$	1.556 (0.448)	1.432 (0.452)	1.279 (0.464)	1.050–1.199 (0.430–0.470) <sup>b</sup>	0.978–1.148 (0.430–0.470) <sup>b</sup>	0.930–1.115 (0.430–0.470) <sup>b</sup>
$g_{Li^+-Cl^-}(r_{M2'})$	1.421–1.083 (0.480–0.530) <sup>b</sup>	1.358–1.088 (0.480–0.530) <sup>b</sup>	1.267–1.097 (0.480–0.530) <sup>b</sup>	1.216 (0.498)	1.201 (0.504)	1.199 (0.508)
$g_{Li^+-Cl^-}(r_{m2})$	0.749 (0.608)	0.756 (0.610)	0.777 (0.614)	0.797 (0.618)	0.816 (0.624)	0.832 (0.630)
$n^{(II)}_{Li^+-Cl^-}(r_{m2})$	6.44 (0.608)	6.27 (0.610)	6.05 (0.614)	5.94 (0.618)	5.95 (0.624)	5.98 (0.630)

Note. For notations, see Table 1. The  $g_{O-O}(r_{M2})$ ,  $g_{O-O}(r_{m2})$ , and  $n^{(II)}_{O-O}(r_{m2})$  values were not determined.

Further heating of the system leads to disappearance of the first minimum of the  $g_{O-O}(r)$  PCF and appearance of an extended plateau instead of the second peak of this PCF. Owing to impossibility of locating the first minimum of this function at  $T > 423$  K, we cannot single out the interactions between the nearest environment and tetrahedrally ordered water molecules. Therefore, in what follows we will use the  $n^{(I+II)}_{O-O}(r_{m2})$  value as a structural characteristic. The value of this parameter is equal to the sum of  $n^{(I)}_{O-O}(r_{m1})$  and  $n^{(II)}_{O-O}(r_{m1})$ . It is determined at a distance corresponding to the position of the second minimum of the

$g_{O-O}(r)$  function. For instance, the LiCl : 14.90 H<sub>2</sub>O solution is characterized by a 9.4% decrease in the  $n^{(I+II)}_{O-O}(r_{m2})$  value in the temperature range 423–523 K.

Changes in the  $g_{O-O}(r)$  PCF of the LiCl : 8.05 H<sub>2</sub>O system with heating are similar to those found for the LiCl : 14.90 H<sub>2</sub>O solution (see Fig. 1 and Table 2). However, it should be noted that in this case the  $g_{O-O}(r)$  function has the first minimum in the whole temperature interval. Raising the temperature to 423 K causes only a 1.5% increase in the  $n^{(I)}_{O-O}(r_{m1})$  value, which is about a quarter as large as that for the

LiCl : 14.90 H<sub>2</sub>O system (see Table 1). The  $n^{(I)}_{O-O}(r_{m1})$  values increases by 7.4% in the temperature interval 298–523 K. In contrast to the less concentrated system, the peak corresponding to the tetrahedral structure of water disappears at a lower temperature (373 K). The  $n^{(II)}_{O-O}(r_{m2})$  value decreases by 10% in the temperature range from 298 to 323 K (see Table 2).

As can be seen in Fig. 1, the  $g_{O-O}(r)$  PCF of the LiCl : 14.90 H<sub>2</sub>O and LiCl : 8.05 H<sub>2</sub>O solutions exhibit no peaks corresponding to the tetrahedral structure of water and have only two well-resolved peaks at 523 K. This shape of the functions is typical of simple liquids with close-packed molecules. The results obtained suggest significant structural rearrangements in the bulk of the solutions upon heating which lead to disappearance of the tetrahedral structure of water. Analogous conclusions were also drawn based on the results of X-ray diffraction study<sup>28</sup> of the structure of neat water in the temperature range from 277 to 473 K and a study of supercritical water by MD simulation.<sup>3</sup>

The  $g_{O-O}(r)$  PCF of the LiCl : 3.15 H<sub>2</sub>O solution, calculated for 298 K exhibits no peak in the region 0.440–0.450 nm. This indicates the absence of tetrahedral ordering of the solvent molecules. A similar shape of the  $g_{O-O}(r)$  function was obtained in MD simulation of the structure of a LiCl solution with the same concentration under standard conditions.<sup>29</sup> The absence of the second peak of this PCF was attributed to essential destruction of the solvent structure in highly concentrated LiCl solutions. A neutron diffraction study of a LiCl solution with a close concentration also revealed the absence of tetrahedral ordering of water molecules at 298 K.<sup>30</sup>

Major changes in the behavior of the  $g_{O-O}(r)$  PCF with heating are similar to those found for the solutions of lower concentrations, but the effect of temperature is less pronounced in this case. For instance, the number of water molecules in the nearest environment increases only by 5.3% in the temperature interval from 298 to 523 K. This is less than one third of the corresponding value for the LiCl : 8.05 H<sub>2</sub>O solution (see Table 3).

The  $g_{O-H}(r)$  PCF of the LiCl : 14.90 H<sub>2</sub>O system, calculated for 298 K, has two clearly seen peaks at  $r = 0.146$  nm and in the region 0.340–0.350 nm (see Fig. 1). The results of MC and MD computer simulation are somewhat different, namely, the first peak of the  $g_{O-H}(r)$  function is shifted toward longer  $r$  ( $r_{M1} \approx 0.180$  nm) while the second maximum is in the region 0.320–0.330 nm. Recently, mention has been made<sup>15</sup> that these distinctions are due to the errors of statistical approximations used in the atom-atom approach (analogous to the RISM approach) rather than the pair potentials used. On the other hand, it is known<sup>31</sup> that the IE method is a reliable tool for obtaining structural information on aqueous electrolyte solutions over a wide range of state parameters.

The higher the concentration of the solution, the lower the intensity of the first peak of the  $g_{O-H}(r)$  PCF. As a consequence, the number of hydrogen bonds,  $n_{O-H}(r_{m1})$ , in the solution decreases with concentration. For instance, this value is only 0.27 for the LiCl : 3.15 H<sub>2</sub>O solution for  $T = 298$  K (see Table 3). This suggests a very low probability of the formation of H-bonds between water molecules in this solution. An analogous conclusion was drawn based on the results of MD simulation of aqueous LiCl solution with a close concentration.<sup>29</sup>

Raising the temperature leads to substantial decrease in the height of the first peak of the  $g_{O-H}(r)$  function of the LiCl : 14.90 H<sub>2</sub>O system, the peak itself being slightly shifted toward shorter  $r$ . The first minimum becomes much shallower and is slightly shifted toward longer  $r$ . As a consequence, the  $n_{O-H}(r_{m1})$  decreases by 11% in the temperature range 298–523 K (see Table 1). For the LiCl : 8.05 H<sub>2</sub>O solution, changes in the shape of the  $g_{O-H}(r)$  PCF are similar, but the effect of temperature is less pronounced. For instance, the  $n_{O-H}(r_{m1})$  value decreases only by 3.4% (see Table 2).

In our previous study of the effect of temperature on the structure of neat water by the IE method we have shown<sup>16</sup> that, despite significant structural rearrangements, increasing the temperature does not lead to complete destruction of hydrogen bonding in water, though the number of H-bonds decreases substantially. These conclusions were also confirmed by the results of MD simulation.<sup>3</sup>

In contrast to the LiCl : 14.90 H<sub>2</sub>O and LiCl : 8.05 H<sub>2</sub>O solutions, the  $g_{O-H}(r)$  PCF of the LiCl : 3.15 H<sub>2</sub>O system behaves in a different manner. Both the intensity and width of its first peak increase with temperature but the peak position is fixed. The first minimum of  $g_{O-H}(r)$  is also characterized by a fixed position; however, it becomes much shallower. These changes lead to a more than 44% increase in the  $n_{O-H}(r_{m1})$  value (see Table 3). Presumably, this is a consequence of very high concentration of the solution.

The  $g_{H-H}(r)$  PCF of the LiCl : 14.90 H<sub>2</sub>O system, calculated for 298 K (see Fig. 1), has two well-resolved peaks at  $r_{M1} = 0.236$  nm and  $r_{M2} = 0.384$  nm. As the LiCl concentration increases, the height of the first peak decreases substantially while the intensity of the second peak remains unchanged, the peaks being shifted in opposite directions.

The intensities of both peaks of the  $g_{H-H}(r)$  PCF of the LiCl : 14.90 H<sub>2</sub>O and LiCl : 8.05 H<sub>2</sub>O solutions decrease as temperature increases. The first maximum is slightly shifted toward shorter while the second maximum is shifted toward longer  $r$ . In contrast to the two less concentrated solutions, changes in the shape of the  $g_{H-H}(r)$  PCF of the LiCl : 3.15 H<sub>2</sub>O system are similar to those found for the  $g_{O-H}(r)$  PCF of the same system,

which can also be due to the very high concentration of the solution.

### ***Ion–water (I–W) correlations***

Considering the  $g_{\text{Li}^+–\text{O}}(r)$ ,  $g_{\text{Li}^+–\text{H}}(r)$ ,  $g_{\text{Cl}^-–\text{O}}(r)$ , and  $g_{\text{Cl}^-–\text{H}}(r)$  PCF calculated for the three systems under study, we noticed that the shapes of the functions belonging to the same group follow common basic patterns and behave analogously with an increase in temperature. Therefore, in Fig. 2 we present only the plots of the  $g_{\text{I}–\text{W}}(r)$  PCF obtained for the  $\text{LiCl} : 14.90 \text{ H}_2\text{O}$  solution. These plots will serve as examples in discussing the effect of temperature on changes in the PCF.

**$\text{Li}^+–\text{O}$ .** The main peak of the  $g_{\text{Li}^+–\text{O}}(r)$  function calculated for 298 K is at  $r = 0.190 \text{ nm}$ , which is in good agreement with the results of experimental and theoretical studies (see, *e.g.*, Refs. 21, 29, and 32). The intensity of the peak depends on concentration of the system and decreases as the concentration increases. This leads to a substantial decrease in the number of water molecules within the first coordination sphere of  $\text{Li}^+$  ion (from 3.44 for  $\text{LiCl} : 14.90 \text{ H}_2\text{O}$  down to 2.51 for the  $\text{LiCl} : 3.15 \text{ H}_2\text{O}$  solution).

Raising the temperature up to 523 K causes a substantial decrease in the intensity of the main peak of the  $g_{\text{Li}^+–\text{O}}(r)$  PCF, though its position remains virtually unchanged (see Fig. 2). The first minimum is noticeably shifted toward longer  $r$  and becomes shallower. These changes in the  $g_{\text{Li}^+–\text{O}}(r)$  function lead to appreciable (by ~30%) decrease in the number of water molecules within the first coordination sphere of  $\text{Li}^+$  ion. For instance, the  $n_{\text{Li}^+–\text{O}}(r_{\text{m1}})$  values are changed from 3.44 to 2.41 for  $\text{LiCl} : 14.90 \text{ H}_2\text{O}$ , from 3.23 to 2.22 for  $\text{LiCl} : 8.05 \text{ H}_2\text{O}$ , and from 2.51 to 1.72 for  $\text{LiCl} : 3.15 \text{ H}_2\text{O}$ .

**$\text{Li}^+–\text{H}$ .** According to our calculations, the  $g_{\text{Li}^+–\text{H}}(r)$  PCF obtained for 298 K has the main peak at  $r_{\text{M1}} = 0.268 \text{ nm}$ . As the concentration of the solution increases, the first peak is slightly shifted toward longer  $r$ . This is accompanied by an increase in the peak intensity. Position of the first maximum of the  $g_{\text{Li}^+–\text{H}}(r)$  function found in this work is in good agreement with the results of computer simulation and neutron diffraction studies of  $\text{LiCl}$  solutions with close concentrations (see, *e.g.*, Refs. 29 and 32).

As in the case of the  $g_{\text{Li}^+–\text{O}}(r)$  functions for all the three solutions under study, the height of the first peak of the  $g_{\text{Li}^+–\text{H}}(r)$  PCF decreases substantially as the temperature increases. The first maximum is shifted toward longer  $r$  while position of the first minimum remains virtually unchanged. According to calculations, the coordination number,  $n_{\text{Li}^+–\text{H}}(r_{\text{m1}})$ , decreases on going from the less to more concentrated solution as temperature increases (from 24.2% for  $\text{LiCl} : 14.90 \text{ H}_2\text{O}$  to 23.1% for  $\text{LiCl} : 3.15 \text{ H}_2\text{O}$ ).

The above-mentioned changes in the shape of the  $g_{\text{Li}^+–\text{O}}(r)$  and  $g_{\text{Li}^+–\text{H}}(r)$  PCF as well as substantial decrease in the  $n_{\text{Li}^+–\text{O}}(r_{\text{m1}})$  and  $n_{\text{Li}^+–\text{H}}(r_{\text{m1}})$  values indicate a decrease in the coordination ability of  $\text{Li}^+$  ion and ordering of water molecules within the first coordination sphere of the  $\text{Li}^+$  ion on heating.

**$\text{Cl}^-–\text{O}$ .** The main peak of the  $g_{\text{Cl}^-–\text{O}}(r)$  PCF of the  $\text{LiCl} : 14.90 \text{ H}_2\text{O}$  system, calculated for 298 K, is at  $r_{\text{M1}} = 0.344 \text{ nm}$  (see Fig. 2). As the concentration increases, the first maximum of this function is slightly shifted toward shorter  $r$  ( $r_{\text{M1}} = 0.342 \text{ nm}$  for  $\text{LiCl} : 3.15 \text{ H}_2\text{O}$ ) and its height increases from 3.536 for  $\text{LiCl} : 14.90 \text{ H}_2\text{O}$  to 3.603 for  $\text{LiCl} : 3.15 \text{ H}_2\text{O}$ . It should be noted that the distances between  $\text{Cl}^-$  ion and O atom of water molecule, obtained in this work for 298 K, are in good agreement with the results obtained by the IE method,<sup>21,31</sup> computer simulation (see, *e.g.*, Refs. 33–36), and in diffraction studies (see, *e.g.*, Ref. 37).

In contrast to "cation–oxygen" PCF, the first minimum of the  $g_{\text{Cl}^-–\text{O}}(r)$  PCF is appreciably shifted toward longer  $r$  as the concentration of the solution increases. However, the  $n_{\text{Cl}^-–\text{O}}(r_{\text{m1}})$  value decreases on going to highly concentrated solutions from 11.47 for  $\text{LiCl} : 14.90 \text{ H}_2\text{O}$  to 9.79 for  $\text{LiCl} : 3.15 \text{ H}_2\text{O}$ . It is known<sup>38</sup> that the coordination number of  $\text{Cl}^-$  ion can vary from 12 to 5 with an increase in the concentration of solution. This suggests a higher mobility of water molecules within the first coordination sphere of  $\text{Cl}^-$  ion compared to that within the first coordination sphere of  $\text{Li}^+$  ion, *i.e.*, weaker interactions of  $\text{Cl}^-$  ions with water molecules.

As in the case of "cation–water" PCF, an increase in temperature up to 523 K leads to pronounced decrease in the height and insignificant broadening of the main peak of the  $g_{\text{Cl}^-–\text{O}}(r)$  PCF irrespective of the solution concentration. Position of the first maximum remains unchanged as the temperature increases. In contrast, the first minimum is appreciably shifted toward longer  $r$ . These changes in the shape of this function correspond to a decrease in the number of water molecules within the first coordination sphere of chloride ion. For instance,  $n_{\text{Cl}^-–\text{O}}(r_{\text{m1}})$  decreases by 5.4% (from 11.47 to 10.85) for  $\text{LiCl} : 14.90 \text{ H}_2\text{O}$ , by 4.7% (from 11.04 to 10.52) for  $\text{LiCl} : 8.05 \text{ H}_2\text{O}$ , and by 8% (from 9.79 to 9.01) for  $\text{LiCl} : 3.15 \text{ H}_2\text{O}$ .

**$\text{Cl}^-–\text{H}$ .** The main peak of the  $g_{\text{Cl}^-–\text{H}}(r)$  PCF calculated for 298 K is at  $r_{\text{M1}} = 0.198 \text{ nm}$  for  $\text{LiCl} : 14.90 \text{ H}_2\text{O}$  and  $\text{LiCl} : 8.05 \text{ H}_2\text{O}$  and at  $r_{\text{M1}} = 0.200 \text{ nm}$  for  $\text{LiCl} : 3.15 \text{ H}_2\text{O}$ . This peak is characteristic of  $\text{Cl}^-–\text{H}$  hydrogen bonds in the systems under study. The  $r_{\text{M1}}$  values found in this work are somewhat different from those obtained by computer simulation (~0.220 nm), which is also due to specific features of the atom-atom approximation.<sup>15</sup> As in the case of the  $g_{\text{O}–\text{H}}(r)$  functions, the height of the first peak of the  $g_{\text{Cl}^-–\text{H}}(r)$  PCF decreases from 4.301 to 4.093 as the solution concentra-

tion increases. This is indicative of reduction of the number of  $\text{Cl}^-$ —H bonds,  $n_{\text{Cl}^--\text{H}}(r_{\text{m}1})$ , from 4.01 for  $\text{LiCl} : 14.90 \text{ H}_2\text{O}$  to 3.14 for  $\text{LiCl} : 3.15 \text{ H}_2\text{O}$ .

For all the systems under study, the heights of the main peaks of the  $g_{\text{Cl}^--\text{H}}(r)$  PCF are nearly halved as the temperature increases. For the  $\text{LiCl} : 14.90 \text{ H}_2\text{O}$  and  $\text{LiCl} : 8.05 \text{ H}_2\text{O}$  solutions, positions of the first maxima remain unchanged while the first minima are shifted toward longer  $r$ . In contrast, the first maximum and minimum of this PCF for  $\text{LiCl} : 3.15 \text{ H}_2\text{O}$  are slightly shifted toward shorter  $r$ . According to calculations, for all the three systems heating up to 523 K is accompanied by a nearly 40% decrease in the number of  $\text{Cl}^-$ —H bonds (from 4.01 to 2.54 for  $\text{LiCl} : 14.90 \text{ H}_2\text{O}$ , from 3.89 to 2.33 for  $\text{LiCl} : 8.05 \text{ H}_2\text{O}$ , and from 3.14 to 1.87 for  $\text{LiCl} : 3.15 \text{ H}_2\text{O}$  solution). On the other hand, the first minimum of the  $g_{\text{Cl}^--\text{H}}(r)$  PCF becomes shallower and the plateau on the  $n_{\text{Cl}^--\text{H}}(r_{\text{m}1})$  plot disappears as the temperature increases. This also suggests a substantial destruction of H-bonds between the  $\text{Cl}^-$  ion and water molecules within its first coordination sphere.

A comparison of changes in the number of water molecules within the first coordination spheres of the cation,  $\Delta n_{\text{Li}^+-\text{O}}(r_{\text{m}1})$ , and anion,  $\Delta n_{\text{Cl}^--\text{O}}(r_{\text{m}1})$ , suggests that heating affects to a greater extent the coordination ability of  $\text{Li}^+$  ion ( $\Delta n_{\text{Cl}^--\text{O}}(r_{\text{m}1}) < \Delta n_{\text{Li}^+-\text{O}}(r_{\text{m}1})$ ).

### Cation-anion ( $\text{Li}^+$ — $\text{Cl}^-$ ) correlations

The plots of the  $g_{\text{Li}^+-\text{Cl}^-}(r)$  PCF are shown in Fig. 3. Irrespective of solution concentration, this function calculated for 298 K has two well-resolved peaks. For all the three solutions, the first peak of  $g_{\text{Li}^+-\text{Cl}^-}(r)$  is at  $r_{\text{M}1} = 0.224 \text{ nm}$ . This peak is determined by the contact interaction between unlikely charged ions ( $\text{Li}^+$ — $\text{Cl}^-$ ). The above-mentioned distance is somewhat shorter than the sum of the ionic radii of  $\text{Li}^+$  and  $\text{Cl}^-$  (0.060 and 0.181 nm, respectively), which is due to the overlap of the electron shells of the ions. Position of the second peak originated from the interaction between the cation and anion separated by a water molecule (a solvent-separated ion pair  $\text{Li}^+-\text{H}_2\text{O}-\text{Cl}^-$ ) depends on concentration of the solution. The  $r_{\text{M}2}$  value is 0.438 nm for  $\text{LiCl} : 14.90 \text{ H}_2\text{O}$  (see Table 1), 0.440 nm for  $\text{LiCl} : 8.05 \text{ H}_2\text{O}$  (see Table 2), and 0.448 nm for  $\text{LiCl} : 3.15 \text{ H}_2\text{O}$  (see Table 3). As a consequence, the  $\text{Li}^+-\text{H}_2\text{O}-\text{Cl}^-$  angle varies from  $106^\circ 37'$  for  $\text{LiCl} : 14.90 \text{ H}_2\text{O}$  to  $111^\circ 30'$  for  $\text{LiCl} : 3.15 \text{ H}_2\text{O}$ . These values are in good agreement with the results of MD simulations,<sup>39</sup> according to which the cation—water—anion angle lies between  $\sim 110$  and  $140^\circ$ . An increase in the concentration is also accompanied by substantial increase in the intensity of the first peak, by a decrease in the intensity of the second peak, and by an appreciable shift of the first and the second minima toward longer  $r$ . These changes in the shape of the

$g_{\text{Li}^+-\text{Cl}^-}(r)$  function suggest an increase in the number of both types of ionic associates in solutions.

As can be seen in the plots of the  $g_{\text{Li}^+-\text{Cl}^-}(r)$  PCF presented in Fig. 3, raising the temperature leads to appreciable increase in the intensity and broadening of the first peaks for the  $\text{LiCl} : 14.90 \text{ H}_2\text{O}$  and  $\text{LiCl} : 8.05 \text{ H}_2\text{O}$  systems. The first maximum and minimum are shifted in opposite directions, toward shorter and longer  $r$ , respectively. Correspondingly, the number of contacts,  $n_{\text{Li}^+-\text{Cl}^-}(r_{\text{m}1})$ , increases substantially (by a factor of 2.5 for  $\text{LiCl} : 14.90 \text{ H}_2\text{O}$  (see Table 1) and by a factor of 1.7 for  $\text{LiCl} : 8.05 \text{ H}_2\text{O}$  (see Table 2)).

As follows from Fig. 3 and the data listed in Table 1 (the  $\text{LiCl} : 14.90 \text{ H}_2\text{O}$  system), there is a shoulder in the region 0.480—0.530 nm on the right side of the second peak with a maximum at  $r = 0.438 \text{ nm}$ . This peak becomes less intense and is appreciably shifted toward longer  $r$  as the temperature increases. At 523 K, the shoulder disappears and the second peak becomes poorly resolved ("diffuse") in the region 0.474—0.480 nm. The second minimum is shifted toward longer  $r$  in the whole temperature range. These changes in the shape of PCF correspond to a 31.7% decrease in the number of solvent-separated ion pairs,  $n_{\text{Li}^+-\text{Cl}^-}(r_{\text{m}2})$ , and to an increase in the  $\text{Li}^+-\text{H}_2\text{O}-\text{Cl}^-$  angle to  $121^\circ 18'$ .

Changes in the shape of the  $g_{\text{Li}^+-\text{Cl}^-}(r)$  function of the  $\text{LiCl} : 8.05 \text{ H}_2\text{O}$  system in the region of the second peak with temperature are similar to the preceding case (see Fig. 3 and Table 2) except that the peak becomes "diffuse" at 473 K. Further heating leads to transformation of the shoulder on the right side of this peak into a peak with a maximum at  $r_{\text{M}2'} = 0.496 \text{ nm}$ , while the initial second peak is transformed into a shoulder in the region 0.430—0.470 nm on the left side of the new peak. The second minimum is appreciably shifted toward longer  $r$  in the whole temperature interval. As a result, the number of solvent-separated ion pairs decreases by 24.6% while the  $\text{Li}^+-\text{H}_2\text{O}-\text{Cl}^-$  angle increases to  $135^\circ 33'$ .

Changes in the shape of the  $g_{\text{Li}^+-\text{Cl}^-}(r)$  PCF of the  $\text{LiCl} : 3.15 \text{ H}_2\text{O}$  solution with heating are different from those found for the other two systems. The main peak of  $g_{\text{Li}^+-\text{Cl}^-}(r)$  becomes much lower, while its width remains virtually unchanged. The first minimum is appreciably shifted toward longer  $r$ . This behavior of the  $g_{\text{Li}^+-\text{Cl}^-}(r)$  function seems to be due to the very high concentration of the solution. As a result, the number of contact ion pairs decreases by 14.1% and the  $\text{Li}^+-\text{Cl}^-$  distance is shortened (see Table 3).

In the region of the second peak, changes in the shape of the  $g_{\text{Li}^+-\text{Cl}^-}(r)$  function are similar to those found for the two less concentrated solutions. The exception is that the shoulder on the right side of the second peak is transformed into an extended peak at 423 K. As temperature increases, the intensity of the

new peak decreases while its maximum and the second minimum continue to shift toward longer  $r$ . In this case, the  $n^{(II)}_{\text{Li}^+ - \text{Cl}^-}(r_{m2})$  value decreases by 7.8% in the temperature interval from 298 to 423 K and then only slightly (by 0.7%) increases on heating from 423 to 523 K. The  $\text{Li}^+ - \text{H}_2\text{O} - \text{Cl}^-$  angle increases to  $145^\circ 19'$ .

A comparison of changes in the number of contact and solvent-separated ion pairs suggests that heating affects to a greater extent the former rather than the latter parameter irrespective of the solution concentration. It should be noted that the decrease in the number of solvent-separated ion pairs and an increase in the number of contact ion pairs in the two less concentrated solutions is in good agreement with the results of MD simulation of related systems.<sup>12</sup>

The results obtained in this work make it possible to draw the following conclusions on the peculiarities of structure formation of concentrated aqueous LiCl solutions under conditions of isobaric heating. An increase in temperature is accompanied by destruction of continuous tetrahedral network of H-bonds between the solvent molecules in the LiCl : 14.90 H<sub>2</sub>O and LiCl : 8.05 H<sub>2</sub>O solutions. Under extreme conditions, hydrogen bonding in these systems is not completely destroyed, though the number of H-bonds decreases substantially; this is in good agreement with the results of MD simulation of neat subcritical and supercritical water.<sup>3</sup> At high temperatures, the three-dimensional structure of water becomes similar to the structure of simple liquids with close-packed molecules. On the other hand, heating leads to an appreciable decrease in the coordination and associative abilities of both ions, the effect of temperature being more pronounced for the cation. The number of contact ion pairs increases substantially while the number of solvent-separated ion pairs decreases as the temperature of solutions increases. We found that heating is to a greater extent responsible for the formation of contact ion pairs rather than for destruction of solvent-separated ion pairs.

Particular emphasis should be placed on the effect of isobaric heating on the structure formation of the LiCl : 3.15 H<sub>2</sub>O solution. Some features of this system are as follows. The tetrahedral network of water molecules is absent already at 298 K. The number of O—H bonds is much less while the number of contact ion pairs is much more than in the two less concentrated systems. In contrast to the LiCl : 14.90 H<sub>2</sub>O and LiCl : 8.05 H<sub>2</sub>O solutions, heating leads to an increase in the number of O—H bonds and to a decrease in the number of contact ion pairs. These features are thought to be due to very high concentration of this solution and will be considered in detail in future studies. Other changes in the structure of the LiCl : 3.15 H<sub>2</sub>O solution under conditions of isobaric heating are similar to those found for the LiCl : 14.90 H<sub>2</sub>O and LiCl : 8.05 H<sub>2</sub>O systems.

This work was carried out with the financial support of the Russian Foundation for Basic Research (Project No. 01-03-32278).

## References

1. H. Ohtaki, T. Radnai, and T. Yamaguchi, *Chem. Soc. Rev.*, 1997, **41**.
2. M. Nakahara, T. Yamaguchi, and H. Ohtaki, *Phys. Chem.*, 1997, **1**, 17.
3. A. G. Kalinichev and J. D. Bass, *J. Phys. Chem.*, 1997, **101**, 9720.
4. P. B. Balbuena, K. P. Johnston, and P. J. Rossky, *J. Phys. Chem.*, 1995, **99**, 1554; 1996, **100**, 2706; 1996, **100**, 2716; *J. Am. Chem. Soc.*, 1994, **116**, 2689.
5. P. H. K. De Jong and G. W. Neilson, *J. Chem. Phys.*, 1997, **107**, 8577.
6. T. Yamaguchi, M. Yamagami, H. Ohzono, K. Yamanaka, and H. Wakita, *Physica B, Condensed Matter*, 1995, **213—214**, 480.
7. Yu. E. Gorbaty and A. G. Kalinichev, *J. Phys. Chem.*, 1995, **99**, 5336.
8. K. Nishikawa and T. Morita, *J. Supercrit. Fluids*, 1998, **13**, 143.
9. L. W. Flanagan, P. B. Balbuena, K. P. Johnston, and P. J. Rossky, *J. Phys. Chem.*, 1995, **99**, 5196.
10. A. V. Okhulkov, Yu. N. Demianets, and Yu. E. Gorbaty, *J. Chem. Phys.*, 1994, **100**, 1578.
11. A. A. Chialvo, P. T. Cummings, J. M. Simonson, and R. E. Mesmer, *Fluid Phase Equil.*, 1998, **150—151**, 2689.
12. S. T. Cui and J. G. Harris, *Chem. Eng. Science*, 1994, **49**, 2749.
13. M. T. Reagan, J. G. Harris, and J. W. Tester, *J. Phys. Chem. B*, 1999, **103**, 7935.
14. B. M. Pettitt and D. F. Calef, *J. Phys. Chem.*, 1987, **91**, 1541.
15. G. Hummer, D. Soumpasis, and M. Neumann, *Mol. Phys.*, 1992, **77**, 769.
16. Yu. V. Kalyuzhnyi, M. V. Fedotova, M. F. Golovko, and V. N. Trostin, *Prepr. Theor. Phys.*, Akad. Sci. Ukr. SSR, Kiev, ITP-N91-19P, 1991, 29 pp. (in Russian).
17. R. D. Oparin, M. V. Fedotova, and V. N. Trostin, *Zh. Obshch. Khim.*, 1998, **68**, 1625 [*Russ. J. Gen. Chem.*, 1998, **68** (Engl. Transl.)].
18. R. D. Oparin, M. V. Fedotova, E. V. Vinogradov, and V. N. Trostin, *Struktura kontsentrirovannykh vodnykh rastvorov khlorida natriya v usloviyakh sil'nogo szhatiya iz dannykh metoda integral'nykh uravnenii* [Structure of Concentrated Aqueous Solutions of Sodium Chloride at High Pressures, as calculated by the method of integral equations], Deposited in and available from VINITI, No. 414-B99 (8.02.99), Moscow, 1999, 10 pp. (in Russian).
19. R. D. Oparin, M. V. Fedotova, and V. N. Trostin, *Izv. Akad. Nauk, Ser. Khim.*, 1999, 1881 [*Russ. Chem. Bull.*, 1999, **48**, 1858 (Engl. Transl.)].
20. R. D. Oparin, M. V. Fedotova, E. V. Vinogradov, and V. N. Trostin, *Struktura kontsentrirovannykh vodnykh rastvorov khlorida kaliya v usloviyakh nagreva pri vysokom davlenii iz dannykh metoda integral'nykh uravnenii* [Structure of Concentrated Aqueous Solutions of Potassium Chloride under Conditions of Heating at High Pressures, as calculated by the method of integral equations], Deposited in and

- available from VINITI, No. 16-B00 (12.01.2000), Moscow, 2000, 13 pp. (in Russian).
21. B. M. Pettitt and P. J. Rossky, *J. Chem. Phys.*, 1986, **84**, 5836.
  22. H. J. C. Berendsen, J. P. M. Postma, W. F. van Gunsteren, and J. Hermans, *Jerusalem Symposium on Quantum Chemistry and Biochemistry*, Ed. B. Pullman, Reidel, Dordrecht, 1981.
  23. B. M. Pettitt and P. J. Rossky, *J. Chem. Phys.*, 1982, **77**, 1451.
  24. D. Chandler and H. C. Andersen, *J. Chem. Phys.*, 1972, **57**, 1930.
  25. Yu. V. Kalyuzhnyi, M. V. Fedotova, M. F. Golovko, and V. N. Trostin, *Prepr. Int. Phys. Condens. Syst.*, Ukr. Akad. Sci., L'vov, 1994, IFKS-93-27-R, 25 pp. (in Russian).
  26. A. H. Narten and W. E. Tissen, *Science*, 1982, **217**, 1033.
  27. G. Palinkas, E. Kalman, and P. Kovacs, *Mol. Phys.*, 1977, **34**, 525.
  28. A. H. Narten, *X-ray Diffraction Data on Liquid Water in the Temperature Range 4-200 °C*, ORNL-4578, 1970, 70 pp.
  29. P. Bopp, I. Okada, H. Ohtaki, and K. Heinzinger, *Z. Naturforsch. A*, 1985, **40**, 116.
  30. B. Prevel, J. F. Jal, J. Dupuy-Philon, and A. K. Soper, *J. Chem. Phys.*, 1995, **103**, 1886.
  31. G. Hummer and D. M. Soumpasis, *Mol. Phys.*, 1992, **75**, 633.
  32. A. H. Narten, F. Vaslow, and H. A. Levy, *J. Chem. Phys.*, 1973, **58**, 5017.
  33. J. Chandrasekhar, W. L. Spellmeyer, and M. L. Jorgensen, *J. Am. Chem. Soc.*, 1984, **106**, 903.
  34. M. Mezei and D. L. Beveridge, *J. Chem. Phys.*, 1981, **74**, 6902.
  35. E. Clementi and R. Barsotti, *Chem. Phys. Lett.*, 1978, **59**, 21.
  36. H. Kistenmacher, H. Popkie, and E. Clementi, *J. Chem. Phys.*, 1974, **61**, 799.
  37. J. E. Enderby and G. W. Neilson, *Rep. Prog. Phys.*, 1981, **44**, 593.
  38. J. P. Limtrakul and B. M. Rode, *Monatsh. Chem.*, 1986, **116**, 1377.
  39. M. Berkowitz, O. A. Karim, J. A. McCammon, and P. J. Rossky, *Chem. Phys. Lett.*, 1984, **105**, 577.

Received August 25, 2000;  
in revised form December 5, 2000